INTERNATIONAL JOURNAL FOR NUMERICAL METHODS IN FLUIDS
Int. J. Numer. Meth. Fluids 2004; **44**:135–146 (DOI: 10.1002/fld.624)

Stability and slightly supercritical oscillatory regimes of natural convection in a 8:1 cavity: solution of the benchmark problem by a global Galerkin method

Alexander Yu. Gelfgat*,†

Department of Fluid Mechanics and Heat Transfer, Faculty of Engineering, Tel-Aviv University, Ramat Aviv, Tel-Aviv 69978, Israel

SUMMARY

The global Galerkin method is applied to the benchmark problem that considers an oscillatory regime of convection of air in a tall two-dimensional rectangular cavity. The three most unstable modes of the linearized system of the Boussinesq equations are studied. The converged values of the critical Rayleigh numbers together with the corresponding oscillation frequencies are calculated for each mode. The oscillatory flow regimes corresponding to each of the three modes are approximated asymptotically. No direct time integration is applied. Good agreement with the previously published results obtained by solution of the time-dependent Boussinesq equations is reported. Copyright © 2004 John Wiley & Sons, Ltd.

KEY WORDS: spectral methods; natural convection; Hopf bifurcation

1. INTRODUCTION

This note is motivated by recently published benchmark results [1] on the calculation of a supercritical oscillatory convective flow. Convection of air ($Pr = 0.71$) in a tall two-dimensional vertical cavity of the aspect ratio height/width $= 8$ was considered. The purpose of the benchmark, as stated in Reference [1] was three-fold: (i) to determine the most accurate estimate of the critical Rayleigh number above which the flow is unsteady, (ii) to identify the correct, i.e. best time-dependent benchmark solution for the 8:1 differentially heated cavity and (iii) to identify those methods that can reliably provide those results.

In this note, we report results obtained using a version of the global Galerkin method [2, 3], which was primarily developed for the purpose of linear stability analysis of numerically

*Correspondence to: A. Yu. Gelfgat, Department of Fluid Mechanics and Heat Transfer, Faculty of Engineering, Tel-Aviv University, Ramat Aviv, Tel-Aviv 69978, Israel.
†E-mail: gelfgat@eng.tau.ac.il

Contract/grant sponsor: Gordon Center for the Energy Studies

Received 5 March 2003
Revised 30 June 2003

calculated flows. This version of the Galerkin method uses non-orthogonal globally defined basis functions, which satisfy all the boundary conditions and the continuity equation. The pressure is excluded by the orthogonal projection of the momentum equation on the divergence-free basis, and the problem reduces to a set of bilinear ODEs, whose steady solutions and linear stability is further studied. The main advantage of this numerical technique is a significant reduction of the number of degrees of freedom of the numerical method, which allows a direct implementation of Newton iteration and QR eigensolver (further details are given in Reference [3]). It is shown that this method accurately reproduces three critical Rayleigh numbers corresponding to the three most unstable perturbation modes computed in the benchmark solution [4]. Among all the results reported (see Reference [1]) the critical Rayleigh number was calculated directly only in References [4, 5], and were estimated in Reference [6]. Here we revalidate these linear stability results.

In the case of the Hopf bifurcation a slightly supercritical oscillatory solution can be asymptotically approximated by the projection on the corresponding central manifold [7]. Such asymptotic approximation was combined with the global Galerkin method in Reference [8], and then was used in References [9, 10] for oscillatory low Prandtl number convection flows in rectangular cavities. The asymptotic approximations were validated against numerical finite-volume solutions of the full time-dependent equations for swirling [8] and convective [3, 9] flows. Moreover, the asymptotic solution computed in Reference [10] yielded a good agreement with experimental results. Here we apply this approach to approximate asymptotically the limit cycles (oscillatory flows) corresponding to the three most unstable perturbation modes. The asymptotic solutions, obtained *without any time integration*, are in a good agreement with the reported benchmark results [1]. Since the present calculations are carried out without time integration and the global Galerkin method needs no discretization of the flow region, the obtained results provide a significant additional validation of the benchmark results. It is stressed, however, that the present numerical approach should be considered as an addition to other methods, and cannot serve as a substitute for the time-dependent calculations unavoidable at large supercriticalities.

Pseudo-spectral approaches were developed recently [11, 12] for the same basis functions as those used in References [2, 3] and here. Using these pseudo-spectral techniques the stability analysis and weakly non-linear approximations can be followed by time-dependent calculations within the same Galerkin approximation.

2. FORMULATION OF THE PROBLEM

Natural convection in a rectangular cavity of width W and height H is considered. The vertical walls of the cavity are maintained at different constant temperatures T_{hot} and T_{cold}, while the horizontal walls are perfectly thermally insulated. The flow is described by the momentum, energy and continuity equations in the Boussinesq approximation. Following Reference [1], we introduce the length scale W, the velocity scale $U=\sqrt{g\beta W(T_{\mathrm{hot}}-T_{\mathrm{cold}})}$, and the scales W/U and ρU^2 for the time and the pressure, respectively. Here g is the acceleration due to gravity, β is the thermal expansion coefficient, and ρ is the density of the fluid. The temperature is rendered dimensionless as in Reference [1] by $\theta=(T-T_{\mathrm{r}})/(T_{\mathrm{hot}}-T_{\mathrm{cold}})$, where $T_{\mathrm{r}}=(T_{\mathrm{hot}}+T_{\mathrm{cold}})/2$. The equations and the boundary conditions, defined in the rectangle

$0 \leqslant x \leqslant 1, 0 \leqslant y \leqslant A$, read

$$\frac{\partial \mathbf{v}}{\partial t} + (\mathbf{v} \cdot \nabla)\mathbf{v} = -\nabla p + \sqrt{\frac{Pr}{Ra}}\Delta \mathbf{v} + \theta \mathbf{j} \tag{1}$$

$$\nabla \cdot \mathbf{v} = 0 \tag{2}$$

$$\frac{\partial \theta}{\partial t} + (\mathbf{v} \cdot \nabla)\theta = \frac{1}{\sqrt{Ra\,Pr}}\Delta \theta \tag{3}$$

$$\text{at } x = 0: \quad \mathbf{v} = \mathbf{0}, \quad \theta = -0.5 \tag{4}$$

$$\text{at } x = 1: \quad \mathbf{v} = \mathbf{0}, \quad \theta = 0.5 \tag{5}$$

$$\text{at } y = 0, A: \quad \mathbf{v} = \mathbf{0}, \quad \frac{\partial \theta}{\partial y} = 0 \tag{6}$$

Here $A = H/W$ is the aspect ratio, $Pr = \nu/\kappa$ is the Prandtl number, $Ra = g\beta(T_{\text{hot}} - T_{\text{cold}})W^3/\nu^2$ is the Rayleigh number; ν is the kinematic viscosity and κ is the thermal diffusivity. The problem is considered for the fixed values $A = 8$ and $Pr = 0.71$ with varying Rayleigh number Ra.

3. NUMERICAL METHOD

The global Galerkin method used here was introduced in Reference [2] and is described in more detail in Reference [3]. Here we recall only several steps of the computational procedure focusing on the benchmark problem considered.

The solution of (1)–(6) is approximated as

$$\mathbf{v} \approx \sum_{i=0}^{N_x}\sum_{j=0}^{N_y} c_{ij}(t)\mathbf{u}_{ij}(x, y), \quad \theta = (x - 0.5) + \sum_{i=0}^{M_x}\sum_{j=0}^{M_y} d_{ij}(t)q_{ij}(x, y) \tag{7}$$

where $c_{ij}(t)$ and $d_{ij}(t)$ are time-dependent coefficients to be found, N_x, N_y, M_x, M_y are numbers of basis functions used for the approximation in the x- and y-directions, respectively; $\mathbf{u}_{ij}(x, y)$ and $q_{ij}(x, y)$ are vector and scalar basis functions. The first term in the representation of θ satisfies the non-homogeneous thermal boundary conditions (4) and (5) along with the homogeneous conditions (6), so that all boundary conditions for $q_{ij}(x, y)$ become homogeneous. The components of the vector basis functions $\mathbf{u}_{ij}(x, y)$ and the scalar basis functions $q_{ij}(x, y)$ are linear superpositions of the Chebyshev polynomials of the first and second kind. The coefficients of these linear superpositions are chosen such that the basis functions satisfy all the homogeneous boundary conditions and the velocity basis is divergence free, i.e. $\nabla \cdot \mathbf{u}_{ij}(x, y) = 0$. Further details and the basis functions for the boundary conditions (4)–(6) can be found in References [2, 3].

The system of ODEs for calculation of the time-dependent coefficients $c_{ij}(t)$ and $d_{ij}(t)$ is obtained by the Galerkin projections of Equations (1) and (3) on the basis functions $\mathbf{u}_{ij}(x, y)$ and $q_{ij}(x, y)$. Note that all the boundary conditions (4)–(6) and the continuity equation (2) are

satisfied before the Galerkin process starts. The orthogonal projection of the pressure gradient on the divergence free basis ($\nabla \cdot \mathbf{u}_{ij} = 0$) satisfying the no-penetration boundary conditions ($\mathbf{u}_{ij} \cdot \mathbf{n} = 0$ at the boundary) gives zero analytically. This can be seen by application of the Gauss integral theorem to

$$\int_\Omega \nabla p \cdot \mathbf{u}_{ij}\, \mathrm{d}\Omega = \int_\Omega [\nabla \cdot (p\mathbf{u}_{ij}) - p\nabla \cdot \mathbf{u}_{ij}]\, \mathrm{d}\Omega = \int_\Omega \nabla \cdot (p\mathbf{u}_{ij})\, \mathrm{d}\Omega = \int_{\partial\Omega} p\mathbf{u}_{ij} \cdot \mathbf{n}\, \mathrm{d}(\partial\Omega) = 0 \quad (8)$$

where Ω is the flow region and $\partial\Omega$ is its boundary. Therefore, the resulting system of ODEs does not contain any algebraic constraint and can be written in the following form (the summation rule over repeating indices is applied)

$$\dot{X}_i = \frac{\mathrm{d}X_i(t)}{\mathrm{d}t} = F_i(\mathbf{X}(t), Ra, Pr, A) = L_{ij}X_j + N_{ijk}X_jX_k + Q_i \quad (9)$$

Here $i, j, k = 1, 2, \ldots, (N_x + 1)(N_y + 1) + (M_x + 1)(M_y + 1)$
and

$$\begin{aligned} X_{i(M_y+1)+j+1} &= d_{ij}, \quad 0 \leqslant i \leqslant M_x; 0 \leqslant j \leqslant M_y \\ X_{(M_x+1)(M_y+1)+i(N_y+1)+j+1} &= c_{ij}, \quad 0 \leqslant i \leqslant N_x; 0 \leqslant j \leqslant N_y \end{aligned} \quad (10)$$

Matrices L_{ij}, N_{ijk}, Q_i contain coefficients of all linear, bilinear and free terms of the equations, respectively, and depend on the governing parameters of the problem.

The steady solutions of the ODE system (9) are calculated by the Newton method. The convergence studies and the validation for convective and swirling flows can be found in References [2, 8–13]. The linear stability analysis of a calculated steady state $\mathbf{X}^0$ reduces to the calculation of the eigenvalues of the Jacobian matrix J_{mk} of the linearized equations (9), which can be expressed as

$$J_{mk} = \frac{\partial \dot{X}_m}{\partial X_k} = L_{mk} + (N_{mkn} + N_{mnk})X_n^0 \quad (11)$$

The eigenvalues are calculated, as a rule, using the QR decomposition algorithm. This algorithm does not depend on the matrix condition number and yields the whole spectrum of the Jacobian matrix. When the dominant eigenvalue is already localized or in cases when a certain single mode is needed (like in the results reported below) the inverse iteration algorithm is applied. The critical Rayleigh number Ra_{cr} corresponds to the change of the sign of the real part of the leading eigenvalue Λ of the Jacobian matrix from negative to positive. It is calculated as a root of the equation $\mathrm{Real}[\Lambda(Ra_{\mathrm{cr}})] = 0$, which is solved by the secant method. Several studies on stability of the calculated convective and rotating flows together with the validations against independent experimental and numerical data are reported in References [2, 3, 8–13].

The last step of the numerical procedure is the non-linear analysis of the calculated bifurcation points. The explicit form of (9) allows one to calculate the projection of the system on the central manifold, which reduces the problem for a slightly supercritical flow to a low-order ODE system (normal form). The solution of this system yields the asymptotic approximation of slightly supercritical solutions. At the moment we have experience carrying out this procedure for Hopf bifurcations, which is the case of the benchmark considered.

In case of the Hopf bifurcation the slightly supercritical oscillatory solution of (9) is approximated asymptotically as [7]

$$Ra = Ra_{\mathrm{cr}} + \mu\varepsilon^2 + O(\varepsilon^4) \tag{12a}$$

$$T(Ra) = \frac{2\pi}{\omega_{\mathrm{cr}}}[1 + \tau\varepsilon^2 + O(\varepsilon^4)] \tag{12b}$$

$$\mathbf{X}(t; Ra) = \mathbf{X}^0(Ra_{\mathrm{cr}}) + \varepsilon Re\left[\mathbf{V}\exp\left(\frac{2\pi i}{T}t\right)\right] + O(\varepsilon^2) \tag{12c}$$

Here $(Ra - Ra_{\mathrm{cr}})$ is the supercriticality, ω_{cr} is the imaginary part of the leading eigenvalue (the critical frequency), T is the period of oscillations, $\mathbf{V}$ is the eigenvector and $\mathbf{X}$ is the asymptotic solution of the ODEs system (9) for the Rayleigh number defined in (12a). The asymptotic expansion (12) is defined by two parameters μ and τ, which can be calculated after the linear stability analysis is completed and the critical parameters Ra_{cr} and ω_{cr} are obtained. The parameters μ and τ are calculated using the algorithm developed in Reference [7]. Details of the application of this algorithm to the ODE system (9) are described in References [3, 8]. The application of Equation (12) proceeds as follows. For a slightly supercritical Rayleigh number Ra the small parameter ε is defined from (12a) as $\varepsilon = \sqrt{(Ra - Ra_{\mathrm{cr}})/\mu}$ (the terms $O(\varepsilon^4)$ in Equations (12a,b) and the term $O(\varepsilon^2)$ in Equation (12c) are neglected). Then the period of oscillations and the oscillatory solutions are obtained from (12b) and (12c), respectively. Note, that the sign of the parameter μ defines whether the Hopf bifurcation is sub- or supercritical.

The asymptotic solutions (12) were validated against time-dependent solutions of the full Navier–Stokes and Boussinesq equations in References [8, 9] and was compared with the experimental observations in Reference [10]. The test calculations performed in Reference [8] showed that the residual of the Navier–Stokes equations remains of the order ε^2 if the supercriticality does not exceed 10%.

The calculations reported below were performed on the ORIGIN 2000 computer using 64 CPUs of type RS10000. A characteristic run that contains all three steps, i.e. calculation of the steady states, linear stability analysis and weakly non-linear analysis of Hopf bifurcation, consumes about 0.375 CPU h/processor for the 20×60 basis functions. With the increase of the number of the basis functions the time increases and is about 0.625 CPU h/processor for 40×100 basis functions.

4. RESULTS

The critical Rayleigh numbers and the critical frequencies calculated at three different truncations of the Galerkin series (7) are shown in Tables I and II. The 'critical frequency' ω_{cr} is the imaginary part of the eigenvalue whose real part crosses zero. This value corresponds to the oscillation frequency in the bifurcation point where the amplitude starts to diverge from zero. It is seen that with the use of 20×80 basis functions in the x- and y-directions, respectively, it is possible to obtain three correct decimal digits of the critical parameters. Furthermore, there is no change in the sixth decimal digits of the critical parameters when the number of basis functions is varied from 30×90 to 40×100. The calculation of the

Table I. Critical Rayleigh number corresponding to the three most unstable perturbation modes.

	20×80 basis functions	30×90 basis functions	40×100 basis functions	Results of Reference [4]
First eigenvalue (mode 1)	306379	306192	306192	306191.6
Second eigenvalue (mode 2)	311314	311234	311234	311169.8
Third eigenvalue (mode 3)	334136	333900	333900	333899.6

Table II. Critical circular frequency corresponding to the three most unstable perturbation modes.

	20×80 basis functions	30×90 basis functions	40×100 basis functions	Results of Reference [4]
First eigenvalue (mode 1)	1.70956	1.70908	1.70908	1.7090841
Second eigenvalue (mode 2)	1.83485	1.83473	1.83473	1.8349204
Third eigenvalue (mode 3)	1.95798	1.95813	1.95813	1.9661282

bifurcation point was assumed to be converged after the first six digits of the critical Rayleigh number remained unchanged. Therefore, we do not report further decimal digits. Comparison with the benchmark results of Reference [4] shows that at least four decimal digits of both solutions coincide, except the frequency of the third mode which was calculated in Reference [4] on a coarser collocation grid.

The fast convergence observed here seems to be common for the spectral methods using the polynomial basis functions. In particular, it was reported for the benchmark problem [1] in References [4, 12, 14]. The divergence-free basis satisfying all the boundary conditions used here and in Reference [12] yields also the conservative properties of the discretized models. It can be shown [3] that for any truncation number the numerical solution satisfies analytically the relations $\langle(\mathbf{v}\cdot)\,\mathbf{v}, \mathbf{v}\rangle = 0$ and $\langle(\mathbf{v}\cdot)\,\theta, \theta\rangle = 0$, where angle brackets represent the inner product with unity weight. It can be shown also that the Galerkin projections of the Laplacian operators result in the negative-definite symmetric matrices. In our opinion, these properties of the discretized model play the decisive role in the fast convergence observed.

Patterns of the flows and the perturbations at the critical values of the Rayleigh number corresponding to modes 1–3 are shown in Figures. 1–3. The patterns of the real and imaginary parts of the temperature perturbations are similar to those reported in Reference [4]. As is pointed out in Reference [4] the real and imaginary parts of modes 1, 2 and 3 consist of 10, 11 and 12 wave structures, respectively. The structures are located near the upper side

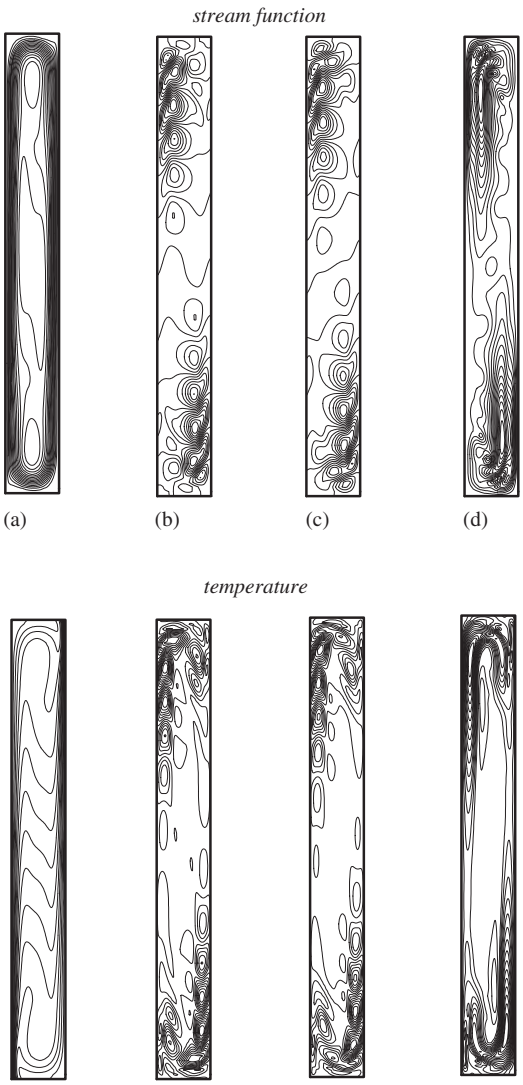

Figure 1. Patterns of the flow and the perturbation at the critical point for mode 1. All isolines are equally spaced: (a) streamlines ($\psi_{\max} = 0.135$) and isotherms; (b) real part of the perturbation; (c) imaginary part of the perturbation; (d) modulus of the perturbation.

of the hot wall and the lower side of the cold one. The perturbation patterns of the stream function contain the same amount of wavy structures located in the same flow regions. The patterns showed in Figure 1 do not coincide completely with those of Reference [4] because the eigenfunctions are defined to within a phase shift (to within multiplication of the complex perturbation vector $\mathbf{V}$ by a complex constant). The phase-independent property, which can be used for comparison of different numerical results, is the modulus of the perturbation. This

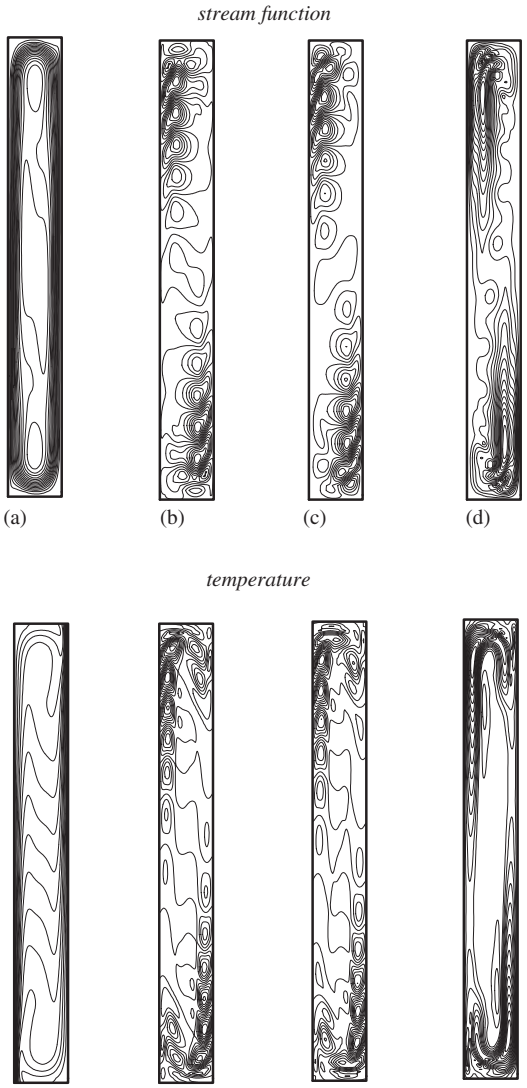

Figure 2. As Figure 1, $\psi_{\max} = 0.134$.

is also included in Figures 1–3. The isolines of the modulus show also that the characteristic width of the temperature perturbation is thinner than that of the velocity.

The parameters μ and τ that define the asymptotic approximation (12) for the supercritical limit cycle were calculated for all three leading perturbation modes. In all three cases the parameter μ was positive, which means that all three limit cycles are supercritical.

We start the description of the asymptotic solutions from the following example. The period of oscillations at $Ra = 3.3 \times 10^5$, developing due to mode 1, is calculated in Reference [4] to be $T = 3.42$. According to the linear stability results the period of oscillations at the critical

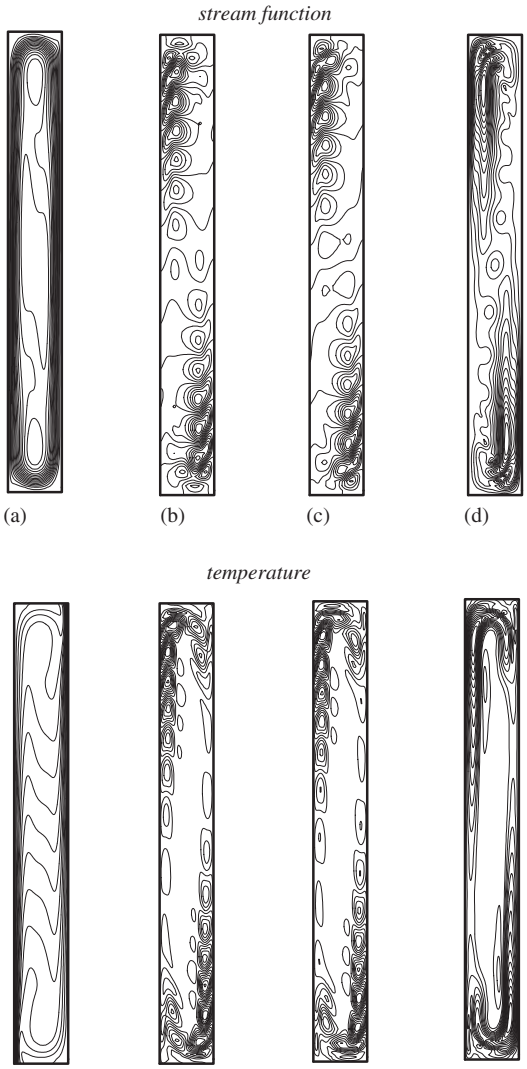

Figure 3. As Figure 1, $\psi_{\max} = 0.131$.

point $Ra_{cr} \approx 3.062 \times 10^5$ is $T_{cr} = 2\pi/\omega_{cr} = 3.676$. Applying the weakly non-linear analysis and calculating the correction to the oscillation period from (12b) we obtain the value $T = 3.417$, which is in a very good agreement with the mentioned result of Reference [4].

The benchmark exercise [1] required to report several characteristic properties of the supercritical oscillatory flow at $Ra = 3.4 \times 10^5$. According to the results of [4, 15] the skew non-symmetric oscillatory flow that develops due to the first instability mode at $Ra_{cr} \approx 3.062 \times 10^5$ is unstable at $Ra = 3.4 \times 10^5$ and the flow switches to the skew symmetric oscillatory regime caused by the growth of mode 2. Since the application of the weakly non-linear analysis does not depend on the stability of a supercritical flow, we calculated the asymptotic approximations

Table III. Characteristic quantities of the oscillatory flow at $Ra = 3.4 \times 10^5$.

Quantity	Present result		Independent results		
	Average	Amplitude	Average	Amplitude	Reference
			First mode		
u_1	0.05720	0.04659			
v_1	0.4535	0.06876			
θ_1	0.2689	0.03891			
ψ_1	0.07070	0.005997			
ω_1	−2.2562	0.9718			
Nu_0	4.4633	0.01070			
Period	3.6480				
			Second mode		
u_1	0.056492	0.052867	0.056345	0.054768	[4]
			0.05634	0.05467	[12]
v_1	0.45498	0.074112	0.46188	0.077125	[4]
			0.46190	0.07700	
θ_1	0.26836	0.043230	0.26548	0.042690	[4]
			0.26552	0.04261	[12]
ψ_1	0.07137	0.0066754	−0.07371	0.00700	[12]
			−0.0737	0.0061	[14]
ω_1	−2.3022	1.05534	−2.37171	1.07555	[12]
			−2.375	0.951	[14]
Nu_0	4.4809	0.007109	4.57946	0.0070921	[4]
			4.57946	0.00708	[12]
Period	3.4113			3.4115	[4]
				3.4012	[12]
			Third mode		
u_1	0.05342	0.02778			
v_1	0.4608	0.03866			
θ_1	0.2660	0.02200			
ψ_1	0.074290	0.003489			
ω_1	−2.5040	0.5141			
Nu_0	4.5585	0.003834			
Period	3.2060				

Table IV. Parameters μ and τ for the second perturbation mode and different number of basis functions.

$N_x \times N_y$	20×60	20×80	30×90	40×100
$\mu/\|\mathbf{V}\|^2 \times 10^7$	1.29047	1.29660	1.29705	1.29724
$\tau/\mu \times 10^9$	−2.37739	−2.37205	−2.37301	−2.37316

of three distinct oscillatory solutions corresponding to the three leading instability modes. The characteristic parameters of these three asymptotic solutions at $Ra = 3.4 \times 10^5$ are reported in Table III. The parameters include the period of oscillations, the mean value and the amplitude of the Nusselt number Nu_0 calculated at the cold wall, and the mean values and the amplitudes of the velocities u_1, v_1, temperature θ_1, stream function ψ_1 and vorticity ω_1 calculated in the point $x_1 = 0.181$, $y_1 = 7.37$. The table contains also the comparison with the solutions of the full time-dependent problem [4, 15].

Obviously, the agreement between the asymptotic and the complete solutions is not as good as that for the critical values (Table III). The main interest is focused on the oscillatory state developing due to mode 2, which is, seemingly, the only one stable at $Ra = 3.4 \times 10^5$ [4, 15]. For this solution the present results differ by less than 4% from the results of Reference [4] and less than 10% from the results of References [12, 15]. Moreover, our asymptotic solutions are within the deviation of other fully non-linear results reported in Reference [1].

Table IV illustrates the convergence of the parameters μ and τ in the asymptotic expansion (12). Note that the values of the parameters depend on the norm of the eigenvector. To eliminate this dependence the parameter μ is scaled by the squared norm of the eigenvector $\mathbf{V}$. Consequently, we report the convergence of the ratio τ/μ rather than the convergence of the parameter τ itself. It is seen that the convergence of these two parameters is slower than that of the critical values. A similar slow down of the convergence was observed also in Reference [8]. The calculation of μ and τ requires calculation of the derivative of the corresponding eigenvalue [8, 13] with respect to the control parameter (the Rayleigh number in the present case), which is carried out by the finite differencing and is the main source of additional numerical error.

5. CONCLUSIONS

The numerical solution of the benchmark problem [1] using the global Galerkin method [3] allowed us to validate the values of the critical Rayleigh numbers and critical frequencies reported in Reference [4]. Application of the weakly non-linear analysis to the calculated Hopf bifurcation yielded additional comparisons with the numerical data obtained by the solution of full time-dependent non-linear problem, thus validating additionally the benchmark results reported in Reference [1]. It should be mentioned that the asymptotic weakly non-linear approximation (12) can be useful not only for comparison purposes. First of all, it gives the pattern of a slightly supercritical oscillatory flow without any time integration of the governing equations [8, 9]. As a rule, the calculation of the parameters μ and τ in (12) takes less CPU time than is needed to complete the linear stability analysis. Besides that, the sign of μ shows whether the bifurcation is sub- or supercritical, which is a very difficult task for any

time-dependent calculation. Finally, a rather good asymptotic approximation of the oscillatory flows may make it possible to perform the Floquet analysis of stability of supercritical oscillatory flows using the asymptotic expansion (12) as a basic state. In this way, for example, the instability of the oscillatory flow developing due to mode 1 can be studied.

ACKNOWLEDGEMENTS

This research was supported by the Gordon Center for the Energy Studies (Tel-Aviv University). The author would like to acknowledge the use of computer resources of the High Performance Computing Unit, a division of the Israel Inter University Computing Center.

REFERENCES

1. Christon MA, Gresho PM, Sutton SB. Computational predictability of time-dependent natural convection flows in enclosures (including benchmark solution). *International Journal for Numerical Methods in Fluids* 2002; **40**:953–980.
2. Gelfgat AYu, Tanasawa I. Numerical analysis of oscillatory instability of buoyancy convection with the Galerkin spectral method. *Numerical Heat Transfer Part A* 1994; **25**:627–648.
3. Gelfgat AYu. Two- and three-dimensional instabilities of confined flows: numerical study by a global Galerkin method. *Computational Fluid Dynamics Journal* 2001; **9**:437–448.
4. Xin S, Le Quéré P. An extended Chebyshev pseudo-spectral benchmark for the 8:1 differentially heated cavity. *International Journal for Numerical Methods in Fluids* 2002; **40**:981–998.
5. Salinger AG, Lehoucq RB, Pawlowski RP, Shadid JN. Computational bifurcation and stability studies of the 8:1 thermal cavity problem. *International Journal for Numerical Methods in Fluids* 2002; **40**:1059–1073.
6. Bruneau C-H, Saad M. From steady to chaotic solutions in a differentially heated cavity of aspect ratio 8. *International Journal for Numerical Methods in Fluids* 2002; **40**:1093–1107.
7. Hassard BD, Kazarinoff ND, Wan Y-H. *Theory and Applications of Hopf Bifurcation*, Mathematical Society Lecture Note Series, vol. 41, London, 1981.
8. Gelfgat A, Bar-Yoseph PZ, Solan A. Stability of confined swirling flow with and without vortex breakdown. *Journal of Fluid Mechanics* 1996; **311**:1–36.
9. Gelfgat AYu, Bar-Yoseph PZ, Yarin AL. Stability of multiple steady states of convection in laterally heated cavities. *Journal of Fluid Mechanics* 1999; **388**:315–334.
10. Gelfgat AYu, Bar-Yoseph PZ, Yarin AL. Non-symmetric convective flows in laterally heated rectangular cavities. *International Journal of Computational Fluid Dynamics* 1999; **11**:261–273.
11. Yahata H. Stability analysis of natural convection in vertical cavities with lateral heating. *Journal of the Physical Society of Japan* 1999; **68**:446–460.
12. Suslov SA, Paolucci S. A Petrov–Galerkin method for flows in cavities: enclosure of aspect ratio 8. *International Journal for Numerical Methods in Fluids* 2002; **40**:999–1007.
13. Gelfgat AYu. Different modes of Rayleigh–Bénard instability in two- and three-dimensional rectangular enclosures. *Journal of Computational Physics* 1999; **156**:300–324.
14. Auteri F, Parolini N. Numerical investigation of the first instabilities in the differentially heated 8:1 cavity. *International Journal for Numerical Methods in Fluids* 2002; **40**:1121–1132.
15. Christopher DM. Numerical prediction of natural convection in a tall enclosure. *International Journal for Numerical Methods in Fluids* 2002; **40**:1039–1044.

